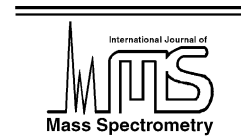




ELSEVIER

International Journal of Mass Spectrometry 223–224 (2003) 91–105



www.elsevier.com/locate/ijms

A selected ion flow tube investigation of the positive ion chemistry of a number of bromine containing fully and partially halogenated hydrocarbons

Chris A. Mayhew^{a,*}, Richard Thomas^{a,1}, Peter Watts^b

^a School of Physics and Astronomy, University of Birmingham, Edgbaston, Birmingham B15 2TT, UK

^b RSG Consulting, Salisbury, Wiltshire SP5 1SP, UK

Received 11 January 2002; accepted 11 March 2002

We wish to dedicate this paper to the memory of Professor W. Lindinger, a greatly respected and admired colleague.

Abstract

The thermal bimolecular rate coefficients and product ion branching ratios for the reactions of the positive ions (in order of increasing recombination energy) H_2O^+ , N_2O^+ , O^+ , CO_2^+ , CO^+ , N^+ , and N_2^+ with the bromine containing molecules CF_3Br , CF_2Br_2 , CFBr_3 , CF_2BrCl , CFBr_2Cl , CBrCl_3 , CH_3Br , CH_2Br_2 , CH_2FBr , CHF_2Br , CH_2BrCl , CHBrCl_2 , CHBr_2Cl , $\text{CF}_3\text{CF}_2\text{Br}$, and $\text{CF}_2\text{BrCF}_2\text{Br}$ at 300 K are reported. This represents the most comprehensive investigation of the positive ion chemistry of brominated molecules to date, with nearly all of the experimental data being presented here for the first time. Also reported in this paper are the reactions of H_2O^+ with $\text{CH}_3\text{CH}_2\text{Br}$, $\text{CH}_2\text{BrCH}_2\text{Cl}$, and $\text{CH}_2\text{BrCH}_2\text{Br}$. All the reactions are efficient, with the experimental reaction rate coefficients being greater than $10^{-9} \text{ cm}^3 \text{ molecule}^{-1} \text{ s}^{-1}$. Dissociative charge transfer is considered to be the dominant reaction mechanism. (Int J Mass Spectrom 223–224 (2003) 91–105)

© 2002 Elsevier Science B.V. All rights reserved.

Keywords: SIFT; Positive ion chemistry; Ion–molecule reaction

1. Introduction

The reactions of ions with neutral molecules play a significant, and often dominant, role in the chemistry of many gaseous plasma environments, including the interstellar medium, planetary ionospheres and industrial plasmas. This has led to many publications reporting ion–molecule reaction rate coefficients and reaction pathways (product ion distributions). See,

for example, the compilation by Ikezoe et al. [1]. Such critical data are invaluable in the understanding of the formation and abundance of ions and neutral molecules present in natural and man-made plasmas, and to predict how such plasmas chemically and physically evolve [2].

There have been many studies investigating the positive ion chemistry of chlorofluorocarbons (CFCs) [1], and a number of studies have explored the positive ion chemistry of their replacements, the perfluorocarbons (PFCs) [3–6]. In part these studies have been undertaken because of their relevance to plasmas, and

* Corresponding author. E-mail: cmayhew@bham.ac.uk

¹ Present address: Department of Physics, Stockholm University, SCFAB, s106 91 Stockholm, Sweden.

are of more specific interest in terms of their relevance to industrial plasma processing. In contrast to fluorinated and/or chlorinated species, little attention has been directed to the reactions of positive ions with bromine containing molecules. Yet systematic studies of these reactions permit useful comparison with the ion chemistry of fully and partially fluorinated/chlorinated compounds. This in turn improves our fundamental understanding of ion–molecule reactions, and ultimately leads, for example, to better models to predict the optimum conditions needed to operate industrial plasma processes.

In this paper we report the rate coefficients and product ion branching ratios for thermal (300 K) reactions of the bromine containing molecules CF₃Br, CF₂Br₂, CFB₃, CF₂BrCl, CFBr₂Cl, CBrCl₃, CH₃Br, CH₂Br₂, CH₂FBr, CHF₂Br, CHFBr₂, CH₂BrCl, CHBrCl₂, CHBr₂Cl, CF₃CF₂Br, and CF₂BrCF₂Br with the following cations (in order of increasing recombination energy): H₂O⁺, N₂O⁺, O⁺, O₂⁺, CO⁺, N⁺, and N₂⁺. In addition to these, the reactions of H₂O⁺ with CH₃CH₂Br, CH₂BrCH₂Cl, and CH₂BrCH₂Br are also presented and discussed in this paper. The majority of this large body of data, representing 115 positive ion reactions with brominated molecules, is being presented here for the first time. Only the reactions of H₂O⁺ with CF₃Br [7,8], and O⁺ with CHF₂Br [9] have been previously reported. Related to this study is a recent study by Španel and Smith [10], who report the reaction rate coefficients and product ion distributions for the reactions of NO⁺ and O₂⁺ with CH₃Br and CH₃CH₂Br.

2. Experimental details

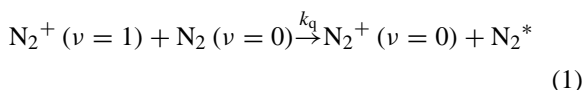
The selected ion flow tube (SIFT) apparatus used in this study to obtain the reaction rate coefficients and product ion branching ratios has been described in detail elsewhere [11,12], so only a brief overview of the salient points of the experimental technique is included here. The reagent ions were generated in an enclosed electron impact high-pressure ion source containing an appropriate gas (N₂ for N₂⁺

and N⁺, CO for CO⁺, CO₂ for CO₂⁺ and O⁺, N₂O for N₂O⁺, and H₂O for H₂O⁺). The reagent ions were mass selected using a quadrupole mass filter, before being injected into a 300 K helium carrier gas at a pressure of ca. 0.5 Torr. The helium gas (of a high-purity grade, 99.997%) was passed through a liquid nitrogen cooled zeolite trap before use. The reagent ions were transported along the flow tube and detected by a downstream quadrupole mass spectrometer detection system. Neutral reactant gas was added in controlled amounts to the ion swarm/carrier gas. All the neutral reactant samples, CF₃Br, CF₂Br₂, CFB₃, CF₂BrCl, CFBr₂Cl, CBrCl₃, CH₃Br, CH₂Br₂, CH₂FBr, CHF₂Br, CHFBr₂, CH₂BrCl, CHBrCl₂, CHBr₂Cl, CH₃CH₂Br, CH₂BrCH₂Cl, CH₂BrCH₂Br, CF₃CF₂Br, and CF₂BrCF₂Br were obtained commercially, and all, except one, with stated purities greater than 95%. The one exception is CFBr₂Cl, which had a stated purity of 90%. Liquids were subjected to several freeze–pump–thaw cycles before use to help to remove dissolved gases. Otherwise all samples were used without further purification.

The loss of the reagent ions and the appearance of product ions were monitored by the detection system. Relaxed resolution on the quadrupole mass spectrometer was used to minimise mass discrimination effects, i.e., the resolution was set to the smallest possible value on the controller which corresponded to mass peaks having a FWHM of about 2 amu. (Higher resolution (>1 amu) was used to assign the peaks in the mass spectra.) This minimises the error in determining the branching ratios. The reaction rate coefficients and ion product distributions were then determined in the usual way [11–13]. Reaction rate coefficients, which were extracted from least-squares fits of the plot of logarithm of the reagent ion signal vs. reactant neutral concentration, are considered to be accurate to ±20%. The percentage product ion branching ratios, determined from the product ion counts as a function of reactant neutral concentration and extrapolated to zero reactant gas concentration to allow for any secondary reactions, are only used to provide a qualitative indication of the important ion channels, and therefore accurate values are not important in

our discussions. However, a statistical analysis on the branching ratios indicates a fractional accuracy of better than 20% for the reaction channels with branching ratios greater than 10%. For ion channels with branching ratios less than this value, the accuracy is reduced.

The high pressure of the gases used in the ionisation source, ca. several Torr, should help to quench electronically and/or vibrationally excited states of molecular ions prior to their injection into the flow tube. We have not made any independent checks to confirm whether these assumptions are correct, other than for N_2^+ , N^+ , and O^+ . For the two atomic ions used in this investigation, N^+ and O^+ , electronically excited states have previously been shown not to be present [5]. For the N_2^+ reagent ion, we know from a previous study that a significant fraction of the N_2^+ ions in the flow tube are vibrationally excited ($\sim 40\%$ in $\nu = 1$) [5]. The rest of the N_2^+ ions are in the ground vibrational state. The vibrationally excited state N_2^+ ions were destroyed in the SIFT tube, prior to them reaching the reaction region. This was achieved by seeding the helium carrier gas with small quantities of N_2 . Lindinger et al. [14] and Smith and Adams [15] have shown that N_2^+ ($\nu > 0$) ions are vibrationally quenched by reactions with N_2 ($\nu = 0$):



with $k_q \sim 4\text{--}6 \times 10^{-10} \text{ cm}^3 \text{ molecule}^{-1} \text{ s}^{-1}$. That no N_2^+ ($\nu = 1$) ions were present in the reaction region of the flow tube was confirmed by the addition of Ar to this region. N_2^+ ($\nu = 1$) efficiently charge transfers to Ar, whereas charge transfer to Ar from N_2^+ ($\nu = 0$) is endothermic. No Ar^+ ions were observed. Whilst it is possible that other reagent molecular ions have internal energies above thermal, no curvature was observed in any of the pseudo-first-order kinetic plots (logarithm of the reagent ion signal vs. the reactant neutral molecule concentration). This indicates that rate coefficients are the same for reactions involving ground and any vibrationally excited states (if present). This does not rule out reagent ion vibrational excitation

influencing the product ion distributions for those reactions which produce more than one product ion.

Water contamination in the flow tube resulted in electron transfer from H_2O to those reagent ions of this study whose recombination energies are greater than the ionisation potential of H_2O , 12.61 eV. The resulting H_2O^+ signal was generally less than 5% of the parent ion signal. Allowances for the reaction of H_2O^+ with the neutral species have been made in the determination of the product ion distributions for all the reactions reported in this paper.

A key aspect of the SIFT technique is the injection of mass-selected ions of a given single m/z ratio into the flow tube. This was not possible for H_2O^+ . Significant quantities of H_3O^+ were produced under the best ion source conditions for H_2O^+ production, and the injection quadrupole mass resolution was not sufficient to reject all the H_3O^+ . In practice, when tuned to inject H_2O^+ , a mixture of 70% H_2O^+ and 30% H_3O^+ was recorded. By use of the SIFT results for H_3O^+ obtained by us [16], the ion products of the reactions of H_2O^+ were readily extracted from the data.

3. Results and discussion

For the purpose of discussion and for convenience of presentation, in this paper the neutral reactants have been placed into one of three groups. Group (i) comprises the fully halogenated methanes, CF_3Br , CF_2Br_2 , CFBr_3 , CF_2BrCl , CFBr_2Cl , and CBrCl_3 . Group (ii) comprises the hydrogenated bromomethanes, CH_3Br , CH_2Br_2 , CH_2FBr , CHF_2Br , CHFBr_2 , CH_2BrCl , CHBrCl_2 , and CHBr_2Cl . $\text{CF}_3\text{CF}_2\text{Br}$ and $\text{CF}_2\text{BrCF}_2\text{Br}$ form the final group, Group (iii).

The experimental rate coefficients, k_{exp} , the observed product ions, and their branching ratios for the reactions of H_2O^+ , N_2O^+ , O^+ , CO_2^+ , CO^+ , N^+ , and N_2^+ with Groups (i)–(iii) are given in Tables 1–3, respectively. In each of the three tables, the reagent ions are listed (top to bottom) in order of increasing recombination energy. The recombination energies of the reagent ions are provided by the numbers in parentheses in eV under the ion formula. Similarly,

Table 1

Reaction rate coefficients, the product ions, and the branching percentages for the reactions of H_2O^+ , N_2O^+ , O^+ , CO_2^+ , CO^+ , N^+ , and N_2^+ with CF_3Br , CF_2Br_2 , CF_2BrCl , CFBr_3 , CFBr_2Cl , and CBrCl_3 at 300 K

	CF_3Br (11.40)	CF_2Br_2 (11.07)	CF_2BrCl (11.21)	CFBr_3 (10.67)	CFBr_2Cl (10.9)	CBrCl_3 (10.60)
H_2O^+ (12.61)	1.6 [1.8] CF_3^+ (71) CF_2Br^+ (16) CF_3Br^+ (8) CF_2OH^+ (5)	1.7 [2.0] CF_2Br^+ (100)	1.7 CF_2Cl^+ (86) CFBrCl^+ (8) CF_2Br^+ (6)	1.8 CFBr_2^+ (100)	1.7 CFBrCl^+ (97) CFBr_2^+ (3)	2.1 [2.1] CCl_3^+ (76) CCl_2Br^+ (24)
N_2O^+ (12.89)	1.1 [1.2] CF_3^+ (100)	1.0 [1.3] CF_2Br^+ (100)	1.2 CF_2Cl^+ (66) CF_2Br^+ (33) CFBrCl^+ (1)	1.2 CFBr_2^+ (100)	1.3 CFBrCl^+ (77) CFBr_2^+ (23)	1.3 [1.4] CCl_2Br^+ (51) CCl_3^+ (49)
O^+ (13.62)	1.6 [1.9] CF_3^+ (91) CF_2Br^+ (9)	1.7 [2.1] CF_2Br^+ (96) CFBr_2^+ (4)	1.7 CF_2Br^+ (50) CF_2Cl^+ (47) CFBrCl^+ (3)	1.7 CFBr_2^+ (95) CFBr^+ (3) CBr_3^+ (2)	1.4 CFBrCl^+ (52) CFBr^+ (48)	1.5 [2.2] CCl_2Br^+ (58) CCl_3^+ (40) CCl_2^+ (2)
CO_2^+ (13.78)	1.1 [1.2] CF_3^+ (99) CF_3Br^+ (1)	1.0 [1.3] CF_2Br^+ (99) CFBr_2^+ (1)	1.2 CF_2Cl^+ (62) CF_2Br^+ (37) CFBrCl^+ (1)	1.4 CFBr_2^+ (99) CBr_3^+ (1)	1.1 CFBrCl^+ (65) CFBr_2^+ (35)	1.2 [1.4] CCl_2Br^+ (59) CCl_3^+ (41)
CO^+ (14.02)	1.3 [1.5] CF_3^+ (89) CF_2Br^+ (11)	1.4 [1.6] CF_2Br^+ (97) CFBr_2^+ (3)	1.4 CF_2Cl^+ (50) CF_2Br^+ (47) CFBrCl^+ (3)	1.4 CFBr_2^+ (94) CFBr^+ (6)	1.3 CFBrCl^+ (62) CFBr_2^+ (37) CBr_2Cl^+ (1)	1.0 [1.7] CCl_2Br^+ (60) CCl_3^+ (39) CCl_2^+ (1)
N^+ (14.54)	1.7 [2.0] CF_3^+ (84) CF_3Br^+ (14) CF_2Br^+ (2)	1.9 [2.2] CF_2Br^+ (97) CFBr_2^+ (3)	1.8 CF_2Cl^+ (85) CF_2Br^+ (12) CFBrCl^+ (3)	2.0 CFBr_2^+ (86) CFBr^+ (12) CBr_3^+ (2)	2.1 CFBrCl^+ (84) CFCl^+ (7) CFBr_2^+ (5) CFBr^+ (3) CBr_2Cl^+ (1)	2.0 [2.3] CCl_3^+ (61) CCl_2Br^+ (31) CCl_2^+ (8)
N_2^+ (15.58)	1.3 [1.5] CF_2Br^+ (74) CF_3^+ (26)	1.4 [1.6] CF_2Br^+ (69) CFBr_2^+ (29) Br_2^+ (2)	1.3 CFBrCl^+ (44) CF_2Br^+ (31) CF_2Cl^+ (25)	1.4 CFBr^+ (91) CFBr_2^+ (8) CBr_3^+ (1)	1.5 CFCl^+ (67) CFBr^+ (25) CFBr_2^+ (4) CFBrCl^+ (3) CBr_2Cl^+ (1)	1.3 [1.7] CCl_2^+ (75) CCl_3^+ (17) CCl_2Br^+ (8)

The reaction rate coefficients, both experimental and calculated (in square brackets), are given in units of $10^{-9} \text{ cm}^3 \text{ molecule}^{-1} \text{ s}^{-1}$. The calculated 300 K Langevin reaction rate coefficients are given for reactant neutral molecules with known polarisabilities [18] or the collisional rate coefficients from parameterised fits to trajectory calculations are given if the polarisability and the dipole moment are both known [17]. Product ion branching percentages are given in parentheses. The recombination energies and ionisation energies of the reagent ions and neutral reactants, respectively, are given in eV in brackets below the relevant species.

Table 2
Reaction rate coefficients, the product ions, and the branching percentages for the reactions of H_2O^+ , N_2O^+ , O^+ , CO_2^+ , CO^+ , N^+ , and N_2^+ with CH_3Br , CH_2Br_2 , CHF_2Br , CHF_2Br_2 , CH_2BrCl , CHBrCl_2 , and CHBr_2Cl at 300 K

	CH_3Br (10.54)	CH_2Br_2 (10.50)	CH_2FBr (10.89)	CHFBr_2 (10.82)	CHF_2Br (11.15)	CH_2BrCl (10.77)	CHBrCl_2 (10.60)	CHBr_2Cl (10.59)
H_2O^+ (12.61)	2.1 [2.7] CH_3Br^+ (90) CH_3BrH^+ (10)	1.6 [2.5] CH_2Br_2^+ (69) CH_2Br^+ (31)	2.0 CH_2FBr^+ (60) CH_2F^+ (36) CH_2Br^+ (4)	2.0 CHFBr^+ (53) CHBr_2^+ (24) CFBr^+ (12) CHFBr_2^+ (11)	2.0 [1.4] CHF_2^+ (76) CHF_2Br^+ (17) CHFBr^+ (7)	2.2 CH_2Cl^+ (63) CH_2BrCl^+ (35) CH_2Br^+ (1) CHBrCl^+ (1)	2.0 CHCl_2^+ (72) CHBrCl^+ (28)	2.0 CHBrCl^+ (91) CHBr_2^+ (7) CHBr_2Cl^+ (2)
N_2O^+ (12.89)	1.5 [1.9] CH_3Br^+ (85) CH_3^+ (15)	1.1 [1.7] CH_2Br^+ (77) CH_2Br_2^+ (14) CHBr_2^+ (9)	1.5 CH_2F^+ (86) CH_2FBr^+ (14)	1.3 CHFBr^+ (100)	1.5 [1.0] CHF_2^+ (96) CHFBr^+ (3) CHF_2Br^+ (1)	1.4 CH_2Cl^+ (95) CH_2BrCl^+ (3) CH_2Br^+ (1) CHBrCl^+ (1)	1.4 CHCl_2^+ (73) CHBrCl^+ (27)	1.4 CHBrCl^+ (90) CHBr_2^+ (9) CHBr_2Cl^+ (1)
O^+ (13.62)	2.4 [2.9] CH_3^+ (74) CH_2Br^+ (15) CH_3Br^+ (11)	1.3 [2.6] CH_2Br^+ (93) CH_2Br_2^+ (7)	2.2 CH_2F^+ (93) CH_2Br^+ (4) CH_2FBr^+ (2) CHFBr^+ (1)	2.2 CHFBr^+ (99) CFBr_2^+ (1)	2.1 [1.5] CHF_2^+ (100)	1.3 CH_2Cl^+ (68) CH_2BrCl^+ (23) CHBrCl^+ (6) CH_2Br^+ (3)	1.6 CHBrCl^+ (51) CHCl_2^+ (30) CHBrCl_2^+ (19)	1.2 CHBrCl^+ (81) CHBr_2^+ (10) CHBr_2Cl^+ (9)
CO_2^+ (13.78)	1.6 [1.9] CH_3^+ (87) CH_3Br^+ (10) CH_2Br^+ (3)	1.1 [1.7] CH_2Br^+ (64) CH_2Br_2^+ (35) CHBr_2^+ (1)	1.5 CH_2F^+ (88) CH_2FBr^+ (6) CH_2Br^+ (6)	1.3 CHFBr^+ (98) CFBr_2^+ (2)	1.3 [1.0] CHF_2^+ (98) CHF_2Br^+ (2)	1.4 CH_2Cl^+ (73) CH_2BrCl^+ (24) CH_2Br^+ (3)	1.3 CHCl_2^+ (75) CHBrCl^+ (24) CHBrCl_2^+ (1)	1.3 CHBrCl^+ (88) CHBr_2^+ (11) CHBr_2Cl^+ (1)

Table 2 (Continued)

	CH ₃ Br (10.54)	CH ₂ Br ₂ (10.50)	CH ₂ FBr (10.89)	CHFBr ₂ (10.82)	CHF ₂ Br (11.15)	CH ₂ BrCl (10.77)	CHBrCl ₂ (10.60)	CHBr ₂ Cl (10.59)
CO ⁺ (14.02)	1.7 [2.3] CH ₃ ⁺ (97) CH ₂ Br ⁺ (3)	1.4 [2.1] CH ₂ Br ⁺ (98) CH ₂ Br ₂ ⁺ (2)	1.7 CH ₂ F ⁺ (95) CH ₂ FBr ⁺ (4) CH ₂ Br ⁺ (1)	1.7 CHFBr ⁺ (98) CFBr ₂ ⁺ (2)	1.7 [1.2] CHF ₂ ⁺ (98) CHFBr ⁺ (1) CHF ₂ Br ⁺ (1)	1.6 CH ₂ Cl ⁺ (72) CH ₂ Br ⁺ (25) CHBrCl ⁺ (3)	1.2 CHBrCl ⁺ (60) CHCl ₂ ⁺ (36) CBrCl ₂ ⁺ (4)	1.3 CHBr ₂ Cl ⁺ (79) CHBr ₂ ⁺ (17) CBr ₂ Cl ⁺ (4)
N ⁺ (14.54)	2.3 [3.0] CH ₃ Br ⁺ (66) CH ₃ ⁺ (29) CH ₂ Br ⁺ (5)	1.5 [2.8] CH ₂ Br ⁺ (72) CH ₂ Br ₂ ⁺ (27) CHBr ₂ ⁺ (1)	2.4 CH ₂ F ⁺ (61) CH ₂ FBr ⁺ (34) CHFBr ⁺ (3) CH ₂ Br ⁺ (2)	2.3 CHFBr ⁺ (93) CFBr ₂ ⁺ (7)	2.3 [1.6] CHF ₂ ⁺ (94) CHF ₂ Br ⁺ (5) CHFBr ⁺ (1)	2.2 CH ₂ Cl ⁺ (81) CH ₂ Br ⁺ (11) CH ₂ BrCl ⁺ (8)	2.2 CHCl ₂ ⁺ (86) CHBrCl ⁺ (14)	2.2 CHBr ₂ Cl ⁺ (86) CHBr ₂ ⁺ (14)
N ₂ ⁺ (15.58)	1.6 [2.3] CH ₃ ⁺ (73) CH ₂ Br ⁺ (21) CHBr ⁺ (6)	1.3 [2.1] CH ₂ Br ⁺ (99) CHBr ₂ ⁺ (1)	1.8 CH ₂ F ⁺ (89) CH ₂ Br ⁺ (5) CH ₂ FBr ⁺ (3) CHF ⁺ (2) CHFBr ⁺ (1)	2.3 CHFBr ⁺ (45) CHF ⁺ (39) CFBr ₂ ⁺ (16)	1.7 [1.2] CHFBr ⁺ (49) CHF ₂ ⁺ (43) CF ₂ ⁺ (2) CFBr ⁺ (2) CF ₂ Br ⁺ (2) CHF ₂ Br ⁺ (2)	1.7 CH ₂ Br ⁺ (61) CH ₂ Cl ⁺ (34) CHCl ⁺ (4) CHBr ⁺ (1)	1.5 CCl ⁺ (68) CHBrCl ⁺ (12) CHCl ₂ ⁺ (10) CHCl ⁺ (8) Br ⁺ (2)	1.7 CHCl ⁺ (30) CCl ⁺ (23) CHBrCl ⁺ (21) CBr ⁺ (18) CHBr ₂ ⁺ (7) CHBr ⁺ (1)

The reaction rate coefficients, both experimental and calculated (in square brackets), are given in units of 10^{-9} cm³ molecule⁻¹ s⁻¹. The calculated 300 K Langevin reaction rate coefficients are given for reactant neutral molecules with known polarisabilities [18] or the collisional rate coefficients from parameterised fits to trajectory calculations are given if the polarisability and the dipole moment are both known [17]. Product ion branching percentages are given in parentheses. The recombination energies and ionisation energies of the reagent ions and neutral reactants, respectively, are given in eV in brackets below the relevant species.

Table 3

Reaction rate coefficients, the product ions, and the branching percentages for the reactions of H_2O^+ , N_2O^+ , O^+ , CO_2^+ , CO^+ , N^+ , and N_2^+ with $\text{CF}_3\text{CF}_2\text{Br}$ and $\text{CF}_2\text{BrCF}_2\text{Br}$ at 300 K

	$\text{CF}_3\text{CF}_2\text{Br}$ (11.65)	$\text{CF}_2\text{BrCF}_2\text{Br}$ (11.10)
H_2O^+ (12.61)	1.9 C_2F_5^+ (68) $\text{CF}_3\text{CF}_2\text{Br}^+$ (26) $\text{C}_2\text{F}_4\text{Br}^+$ (4) CF_2Br^+ (2)	2.0 $\text{CF}_2\text{CF}_2\text{Br}^+$ (92) $\text{CF}_2\text{BrCF}_2\text{Br}^+$ (5) CF_2Br^+ (3)
N_2O^+ (12.89)	1.2 C_2F_5^+ (92) CF_2Br^+ (6) $\text{CF}_3\text{CF}_2\text{Br}^+$ (2)	1.3 $\text{CF}_2\text{CF}_2\text{Br}^+$ (89) CF_2Br^+ (10) $\text{CF}_2\text{BrCFBr}^+$ (1)
O^+ (13.62)	1.7 C_2F_5^+ (91) CF_2Br^+ (7) CF_3^+ (2)	1.5 $\text{CF}_2\text{CF}_2\text{Br}^+$ (70) CF_2Br^+ (29) C_2F_4^+ (1)
CO_2^+ (13.78)	1.2 C_2F_5^+ (94) CF_2Br^+ (4) CF_3^+ (1) $\text{CF}_3\text{CF}_2\text{Br}^+$ (1)	1.2 $\text{CF}_2\text{CF}_2\text{Br}^+$ (69) CF_2Br^+ (29) $\text{CF}_2\text{BrCF}_2\text{Br}^+$ (1) $\text{CF}_2\text{BrCFBr}^+$ (1)
CO^+ (14.02)	1.4 C_2F_5^+ (87) $\text{C}_2\text{F}_4\text{Br}^+$ (6) CF_2Br^+ (5) CF_3^+ (1) $\text{CF}_3\text{CF}_2\text{Br}^+$ (1)	1.0 $\text{CF}_2\text{CF}_2\text{Br}^+$ (55) CF_2Br^+ (40) $\text{CF}_2\text{BrCFBr}^+$ (3) C_2F_4^+ (1) $\text{CF}_2\text{BrCF}_2\text{Br}^+$ (1)
N^+ (14.54)	1.8 C_2F_5^+ (56) $\text{CF}_3\text{CF}_2\text{Br}^+$ (29) CF_2Br^+ (6) $\text{C}_2\text{F}_4\text{Br}^+$ (6) CF_3^+ (3)	2.0 $\text{CF}_2\text{CF}_2\text{Br}^+$ (67) CF_2Br^+ (26) C_2F_4^+ (6) $\text{CF}_2\text{BrCF}_2\text{Br}^+$ (1)
N_2^+ (15.58)	1.3 $\text{C}_2\text{F}_4\text{Br}^+$ (47) CF_3^+ (31) C_2F_5^+ (12) CF_2Br^+ (9) $\text{CF}_3\text{CF}_2\text{Br}^+$ (1)	1.3 CF_2Br^+ (64) $\text{CF}_2\text{BrCFBr}^+$ (28) C_2F_4^+ (8)

The experimental rate coefficients are given in units of $10^{-9} \text{ cm}^3 \text{ molecule}^{-1} \text{ s}^{-1}$. Product ion branching percentages are given in parentheses. The recombination energies and ionisation energies of the reagent ions and neutral reactants, respectively, are given in eV in brackets below the relevant species.

the ionisation potentials of the neutral reactants are also listed in the tables, again in parentheses in eV under the neutral molecular formula. The ionisation potentials of CHF_2Br and $\text{CF}_3\text{CF}_2\text{Br}$ have had to

be estimated from the ionisation potential of similar molecules.

A comparison of the experimental rate coefficients, k_{exp} , with the capture values, k_{c} , provides a good indication of whether a reaction is efficient ($k_{\text{exp}} \sim k_{\text{c}}$), with most captures leading to reaction, or inefficient ($k_{\text{exp}} \ll k_{\text{c}}$). Essential pieces of information for making capture theory calculations of k_{c} are the polarisability and the dipole moment of the neutral reactant molecule. Given these values the capture rate coefficients can be estimated using the results of parameterised fits to trajectory calculations [17]. If only the polarisability is known the Langevin rate coefficients may be determined [18]. For the Group (i) molecules, the polarisabilities and dipole moments are only available for CF_3Br , CF_2Br_2 , and CBrCl_3 . For the Group (ii) molecules, the polarisabilities and dipole moments are known for CH_3Br and CH_2Br_2 , and only the polarisability for CHF_2Br is available. For those reactions for which k_{c} can be determined, the value appears in square brackets in Tables 1 and 2. The polarisabilities and dipole moments of Group (iii) molecules, $\text{CF}_3\text{CF}_2\text{Br}$ and $\text{CF}_2\text{BrCF}_2\text{Br}$, are unknown, and hence no k_{c} values are given for the reactions of the ions with these two molecules. Most of the polarisabilities and dipole moments have been taken from the CRC Handbook [19]. The polarisability of CF_3Br (6.78 \AA^3) has been taken from the work of Morris [20], the polarisability (12.0 \AA^3) and dipole moment (0.2 D) of CBrCl_3 have been taken from the work of Knighton and Grimsrud [21].

The determination of reaction pathways requires knowledge of the ion and neutral products. In our experiments, the masses and relative yields of the ion products are determined, so the neutral products can only be inferred from mass balance and thermochemical arguments. The thermochemical analysis is restricted to considerations of enthalpy (i.e., $\Delta H < 0$ for an observable reaction). Paucity of relevant thermodynamic data has, as usual, restricted our thermodynamic analysis to considerations of enthalpy rather than free energy, although we appreciate that entropic effects may be important in driving a reaction that is thermoneutral or slightly endoergic.

Unless otherwise stated, the enthalpy of the reactions presented in the text have been calculated using enthalpies of formation from the NIST website [22], supplemented with data from the tables of Lias et al. [23].

3.1. The Group (i) molecules: the fully halogenated methane

This section presents the results and thermochemical analysis of the reactions of H_2O^+ , N_2O^+ , O^+ , CO_2^+ , CO^+ , N^+ , and N_2^+ with the bromine containing fully halogenated methanes, comprising Group (i). Table 1 presents the experimental rate coefficients, k_{exp} , and the product ion branching ratios. The reagent ions are arranged in order of increasing recombination energy, and the neutral reactant molecules in order of decreasing fluorination; CF_3Br to CBrCl_3 . The ionisation potentials of the brominated molecules are given in brackets in eV under the molecular formula. Only the ionisation potential of CFBr_2Cl is not available in the literature. The quoted value of $I(\text{CFBr}_2\text{Cl}) = 10.9 \text{ eV}$ has been estimated from $I_{\text{P}}(\text{CFBr}_3) = 10.67 \text{ eV}$ and the observation that replacing Br by Cl increases the ionisation potential by $\sim 0.20 \text{ eV}$, a value obtained by comparing the ionisation potentials of the pairs of molecules $\text{CF}_2\text{Br}_2/\text{CF}_2\text{BrCl}$ (0.23 eV), $\text{CH}_2\text{Br}_2/\text{CH}_2\text{BrCl}$ (0.27 eV), and $\text{CHBr}_3/\text{CHBr}_2\text{Cl}$ (0.11 eV).

CF_3Br has been the subject of a series of positive ion chemistry investigations by Morris et al. They studied the reactions of CF_3Br with HCO^+ , CH_3^+ , and CH_5^+ [24], Ar^+ [25], H_2O^+ [7], and CF_3^+ [26]. We have also previously published some investigations on the positive ion chemistry of the Group (i) molecules; namely the reactions of H_3O^+ and H_2O^+ [8]. For convenience, the results of the reactions with H_2O^+ are reproduced and briefly summarised in this paper.

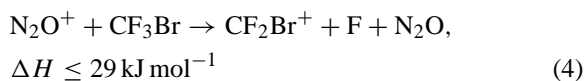
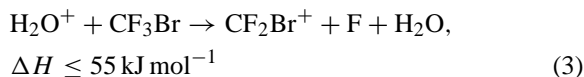
All the fully halogenated brominated molecules react with H_2O^+ efficiently and predominantly by dissociative charge transfer, via a short-range interaction. The evidence for a short-range interaction comes from the small Franck–Condon factors connecting the

ground state of a fully halogenated bromomethane to an ionic state at the recombination energy of H_2O^+ [27–30]. Further evidence to support this short-range mechanism comes from the observation of CF_2OH^+ as an ion product (5%) from the reaction of H_2O^+ with CF_3Br . This product ion can only result from a chemical reaction occurring within an ion–molecule complex.

For the other reagent ions used in this study (N_2O^+ , O^+ , CO_2^+ , CO^+ , N^+ , and N_2^+), dissociative charge transfer is also observed to be the dominant reaction mechanism. The overall process can be viewed as a two-step mechanism, transfer of an electron from the reactant neutral (MX) to the reagent ion (A^+), followed by fragmentation of the unstable intermediate ion, $[\text{MX}^+]^*$:



where $\text{X} = \text{F}, \text{Cl}$ or Br . Table 4 collects the enthalpies of reaction for all of the dissociative charge transfer pathways leading to a trihalomethyl cation. In compiling this table, the following experimentally established upper limits to the enthalpies of formation of observed carbocation products have been used: $\Delta_{\text{f}}H(\text{CF}_2\text{Br}^+) < 544 \text{ kJ mol}^{-1}$ [31], $\Delta_{\text{f}}H(\text{CF}_2\text{Cl}^+) < 506 \text{ kJ mol}^{-1}$ [7], and $\Delta_{\text{f}}H(\text{CBr}_3^+) < 869 \text{ kJ mol}^{-1}$, $\Delta_{\text{f}}H(\text{CFBr}_2^+) < 633 \text{ kJ mol}^{-1}$, $\Delta_{\text{f}}H(\text{CFBrCl}^+) < 667 \text{ kJ mol}^{-1}$, $\Delta_{\text{f}}H(\text{CBr}_2\text{Cl}^+) < 924 \text{ kJ mol}^{-1}$, and $\Delta_{\text{f}}H(\text{CCl}_2\text{Br}^+) < 882 \text{ kJ mol}^{-1}$ [8]. With the possible exception of two reactions:



these fragmentation pathways to the trihalomethyl cations are all exothermic. It is not possible to rule out that the product ion CF_2Br^+ resulting from the reactions with H_2O^+ and N_2O^+ is produced through a chemical (more exothermic) reaction pathway, for example:

Table 4

Compilation of the upper limits of the reaction enthalpies for the dissociative charge transfer reaction pathways $A^+ + MX \rightarrow [MX^+]^* + A \rightarrow M^+ + X + A$, $X = F, Cl$ or Br , for the fully halogenated methane group of molecules CF_3Br , CF_2Br_2 , $CFBr_3$, CF_2BrCl , $CFBr_2Cl$, and $CBrCl_3$

MX	X	Reagent cation A ⁺						
		H ₂ O ⁺	N ₂ O ⁺	O ⁺	CO ₂ ⁺	CO ⁺	N ⁺	N ₂ ⁺
		Upper limits to the reaction enthalpy for dissociative charge transfer (kJ mol ^{−1})						
CF ₃ Br	Br ^a	−57	−83	−154	−169	−193	−242	−343
	F	55	29	−42	−57	−81	−130	−231
CF ₂ Br ₂	Br	−182	−208	−279	−294	−318	−367	−468
	F	−126	−152	−223	−238	−262	−311	−412
CFBr ₃	Br	−236	−262	−333	−348	−372	−421	−552
	F	−33	−59	−130	−145	−169	−218	−319
CF ₂ BrCl	Br	−161	−187	−258	−273	−297	−346	−447
	Cl	−114	−140	−211	−226	−250	−299	−400
	F	−33	−59	−130	−145	−169	−218	−319
CFBr ₂ Cl	Br	−257	−283	−354	−369	−393	−442	−543
	Cl	−282	−308	−379	−394	−417	−467	−568
	F	−33	−59	−130	−145	−169	−218	−319
CBrCl ₃	Br	−231 ^b	−257	−328	−343	−367	−416	−517
	Cl	−171	−197	−268	−283	−307	−356	−457

^a The reaction enthalpies for the reaction of the reagent ions with CF_3Br leading to the elimination of Br are the actual reaction enthalpies and not upper limits.

^b This is the actual reaction enthalpy for the reaction of H_2O^+ with $CBrCl_3$ leading to the products CCl_3^+ , Br and H_2O .



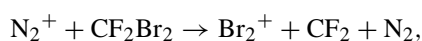
$$\Delta H \leq -15 \text{ kJ mol}^{-1} \quad (5)$$

In addition to the trihalomethyl product cation, a number of the reactions result in other product cations. Non-dissociative charge transfer is observed for the reactions of H_2O^+ (8%), CO_2^+ (1%) and N^+ (14%) with CF_3Br . A threshold photoelectron–photoion coincidence (TPEPICO) study of CF_3Br [32] shows virtually no yield for CF_3Br^+ much above photon energies of 12 eV. That CF_3Br^+ is an observed product for reactions involving these above three reagent ions is another indication of a short-range interaction taking place leading to the formation of an ion–molecule complex. Such a short-range interaction is clearly apparent for the reaction of H_2O^+ with CF_3Br because of the observation of the protonated carbonic dihalide, CF_2OH^+ :



$$\Delta H = -267 \text{ kJ mol}^{-1} \quad (6)$$

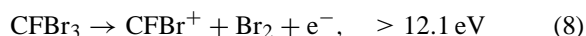
An interesting product ion is observed from the reaction of N_2^+ with CF_2Br_2 , namely Br_2^+ is observed as a minor ion product (2%) via dissociative charge transfer:



$$\Delta H = -283 \text{ kJ mol}^{-1} \quad (7)$$

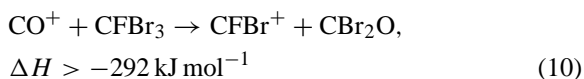
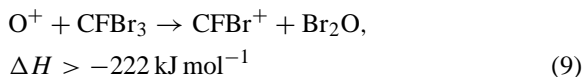
This is the only reaction which produces this unusual product ion, resulting from the breaking of two C–Br bonds and the formation of a Br–Br bond.

For $CFBr_3$, $CFBr^+$ is observed as a product ion for the reactions with O^+ , CO^+ , N^+ , and N_2^+ . $\Delta_f H(CFBr^+)$ is unknown, but it will be greater than $\Delta_f H(CF_2^+) = 897 \text{ kJ mol}^{-1}$. Using this value the following dissociation energy can be estimated:

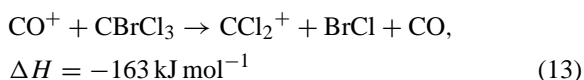
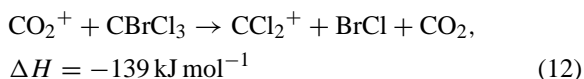
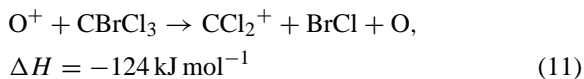


Reaction (8) is energetically available to all of the reagent ions, but is not observed for the reactions with H_2O^+ , N_2O^+ , and CO_2^+ . The production of $CFBr^+$

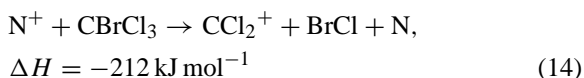
from the reactions with O^+ and CO^+ may thus be a result of a chemical interaction, for example:



CCl_2^+ is an observed product ion from the reactions of O^+ , CO_2^+ , CO^+ , and N^+ with $CBrCl_3$. Using $\Delta_f H(CCl_2^+) = 1133 \text{ kJ mol}^{-1}$, calculated from $\Delta_f H(CCl_2) = 239 \text{ kJ mol}^{-1}$ and the ionisation potential of CCl_2 , 9.27 eV, the energy required to form $CCl_2^+ + Br + Cl + e^-$ from $CBrCl_3$ is 14.6 eV. Within the uncertainties associated with this value, the dissociation channel may be accessible for the reaction with N^+ , but is not accessible for the reactions with O^+ , CO_2^+ , and CO^+ . Instead, $BrCl$ must be formed to make the dissociative charge transfer channel exothermic:



and possibly



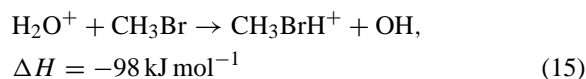
As discussed above, for the majority of the reactions dissociative charge transfer is considered to be the dominant and efficient reaction mechanism for reactions with this group of molecules. For several of the reactions there is clear evidence that an ion–molecule complex is formed and that charge transfer is occurring through a short-range mechanism, which may be competing with chemical reaction pathways. Evidence

in support of the short-range dissociative charge transfer channels comes from the photoelectron spectra of CF_3Br [27], CF_2Br_2 [28], $CFBr_3$ [29], CF_2BrCl [28], and $CBrCl_3$ [30]. (No photoelectron spectrum exists in the literature for $CFBr_2Cl$.) An inspection of these photoelectron spectra shows that for the majority of the reactions, there are no accessible ionic states with good Franck–Condon factors at the recombination energies of the reagent ions. The exceptions are the reactions of O^+ , CO_2^+ , CO^+ and N_2^+ with CF_3Br , N_2^+ with CF_2Br_2 , N_2O^+ , CO_2^+ , and CO^+ with CF_2BrCl , and CO_2^+ and CO^+ with $CFBr_3$, for which good intensities in the respective photoelectron spectra exist at the recombination energies of these reagent cations, and hence dissociative charge transfer could be occurring via a long-range mechanism for these reactions [33].

3.2. The Group (ii) molecules: the hydrogenated bromomethane

This section presents the results and thermochemical analysis of the reactions of H_2O^+ , N_2O^+ , O^+ , CO_2^+ , CO^+ , N^+ , and N_2^+ with the following hydrogenated bromomethanes: CH_3Br , CH_2Br_2 , CH_2FBr , CHF_2Br , $CHFBr_2$, CH_2BrCl , $CHBrCl_2$, and $CHBr_2Cl$. Of these reactions only that of O^+ with CHF_2Br has been previously investigated [9]. Table 2 presents the experimental rate coefficients, k_{exp} , and the product ion branching ratios. All reactions are efficient with $k_{\text{exp}} \sim k_c$, and the major reaction mechanism is considered to be charge transfer. Non-dissociative and dissociative charge transfer are both observed. Only for the reactions with $CHBrCl_2$ is the non-dissociative charge transfer channel leading to the formation of the parent ion not observed. For the reactions with $CHFBr_2$ and $CHBr_2Cl$, the non-dissociative channel is only observed from the reaction with H_2O^+ , and then only as a minor product ion, 11 and 2%, respectively.

For the reaction of H_2O^+ with CH_3Br proton transfer competes with non-dissociative charge transfer:



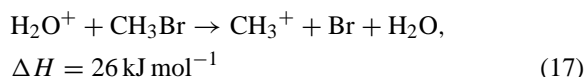
The non-dissociative charge transfer channel is also observed for the reactions of other reagent ions with CH_3Br , with the branching ratio decreasing with increasing recombination energy of the reagent ion, starting with 90% for the reaction with H_2O^+ (RE = 12.61 eV) and reaching 0% for the reaction with CO^+ (RE = 14.02 eV), whilst the branching ratio for CH_3^+ is increasing, from 0% (H_2O^+) to 97% (CO^+). There is a dramatic reversal to this trend for the reaction with N^+ (RE = 14.54 eV) when the CH_3Br^+ parent ion becomes the dominant product ion (66%). Španel and Smith [10] report that only CH_3Br^+ is observed from the reaction with O_2^+ . This agrees with our observations in that the recombination energy of O_2^+ (12.07 eV) is less than that of H_2O^+ . The observation of CH_3^+ as the dominant ion for a number of the reactions agrees with a state selected study of CH_3Br^+ by Lane and Powis [34]. They report that only the ground ionic state of CH_3Br is stable against dissociation, with the excited ionic states preferentially fragmenting to CH_3^+ (with a threshold of 12.80 ± 0.03 eV). The recombination energy of all the reagent ions lie well above the ground electronic state of CH_3Br^+ [35]. The observation of CH_3Br^+ from the reactions with H_2O^+ and N_2O^+ can be explained from their recombination energies, which are either just below (H_2O^+) or are just on (N_2O^+) the onset of the first excited ionic state of CH_3Br . Thus, long-range charge transfer, which is expected to result in similar product ions as obtained from threshold photoionisation using photons with energies equal to the recombination energies of the reagent ions, is likely to be inoperative, and the charge transfer takes place by a short-range mechanism within an ion–molecule complex. Under these circumstances a one-to-one correspondence of the ion branching ratios obtained from ion–molecule reactions and photoionisation studies is not to be expected.

It might be at first expected the O^+ would react with these hydrogenated compounds by hydrogen abstraction. However, a glance at Table 2 shows that dissociative charge transfer is the dominant reaction mechanism not only for the reactions with O^+ , but with all the reagent ions. Often more than one disso-

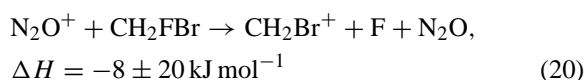
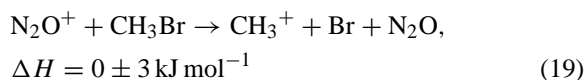
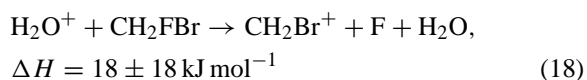
ciation limit is available at the recombination energy of the reagent ion:



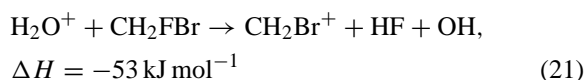
where X = H, F, Cl or Br. Table 5 collects the enthalpies of reaction for all of the dissociative charge transfer pathways. In compiling this table, the following have been used: $\Delta_f H(\text{CF}_2\text{Br}^+) \leq 544 \text{ kJ mol}^{-1}$ [31], $\Delta_f H(\text{CFBr}_2^+) \leq 633 \text{ kJ mol}^{-1}$ [8], $\Delta_f H(\text{CHBrCl}^+) \leq 876 \text{ kJ mol}^{-1}$, $\Delta_f H(\text{CHFBr}^+) \leq 688 \text{ kJ mol}^{-1}$, and $\Delta_f H(\text{CHBr}_2^+) \leq 924 \text{ kJ mol}^{-1}$, from our recent study of the reactions of H_3O^+ with this group of molecules [16]. From Table 5 it can be seen that dissociative charge transfer is an exothermic channel to the various methyl cations. The only exceptions to this are



and possibly



Alternatively, an intimate chemical reaction is occurring, for example:



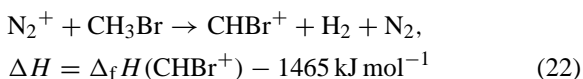
The dissociative charge transfer channels observed only for the reactions of N_2^+ , which do not follow the reaction pathway (16). The product ions of these channels are as follows: CHBr^+ (6%) from the reaction with CH_3Br ; CCl^+ (68%), CHCl^+ (8%) and Br^+ (2%) from the reaction with CHBrCl_2 ; CHF^+ from the reactions with CH_2FBr (2%) and CHFBr_2 (39%); CF_2^+

Table 5

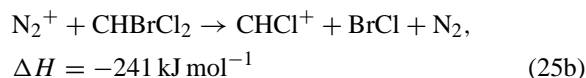
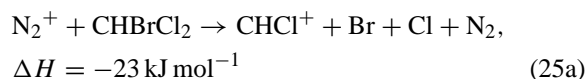
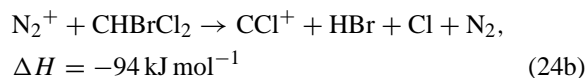
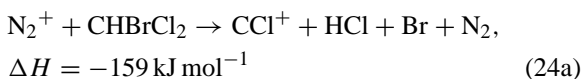
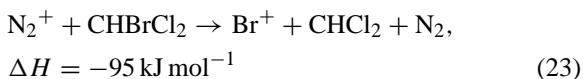
Compilation of the reaction enthalpies for the dissociative charge transfer reaction pathways $A^+ + MX \rightarrow [MX^+]^* + A \rightarrow M^+ + X + A$, $X = H, F, Cl$ or Br , for the hydrogenated bromomethane group of molecules CH_3Br , CH_2Br_2 , CH_2FBr , CHF_2Br , $CHFBr_2$, CH_2BrCl , $CHBrCl_2$, $CHBr_2Cl$

MX	X	Reagent cation A ⁺						
		H ₂ O ⁺	N ₂ O ⁺	O ⁺	CO ₂ ⁺	CO ⁺	N ⁺	N ₂ ⁺
		Upper limits to the reaction enthalpy for dissociative charge transfer (kJ mol ^{−1})						
CH ₃ Br	Br	26	0 ± 3	−71	−86	−110	−159	−260
	H	−24	−50	−121	−136	−160	−209	−310
CH ₂ Br ₂	Br	−168	−194	−265	−280	−304	−353	−454
	H	−75	≤−101	≤−172	≤−187	≤−211	≤−260	≤−361
CH ₂ FBr	Br	−53	−79	−150	−165	−189	−238	−339
	F	18 ± 18	−8 ± 20	−79	−94	−118	−167	−268
	H	≤−92	≤−118	≤−189	≤−204	≤−228	≤−277	≤−378
CHF ₂ Br	Br	−69	−95	−166	−181	−205	−254	−355
	F	≤−25	≤−51	≤−122	≤−137	≤−161	≤−210	≤−311
	H	≤−30	≤−56	≤−127	≤−142	≤−156	≤−215	≤−316
CHFBr ₂	Br	≤−236	≤−262	≤−333	≤−348	≤−372	≤−421	≤−522
	F	−33	≤−59	≤−130	≤−145	≤−169	≤−218	≤−319
	H	≤−185	≤−211	≤−282	≤−297	≤−321	≤−370	≤−471
CH ₂ BrCl	Br	−191	−217	−288	−304	−326	−376	−477
	Cl	−204	−230	−301	−316	−340	−389	−490
	H	≤−168	≤−194	≤−265	≤−280	≤−304	≤−353	≤−454
CHBrCl ₂	Br	−169	−195	−266	−281	−305	−354	−455
	Cl	≤−171	≤−197	≤−268	≤−283	≤−307	≤−356	≤−457
	H	≤−68	≤−94	≤−165	≤−180	≤−204	≤−253	≤−354
CHBr ₂ Cl	Br	≤−238	≤−264	≤−335	≤−350	≤−374	≤−423	≤−524
	Cl	−181	≤−207	≤−278	≤−293	≤−317	≤−366	≤−467
	H	≤−84	≤−110	≤−181	≤−196	≤−220	≤−269	≤−370

(2%) from the reaction with CHF_2Br . The exothermicities of these pathways are as follows, starting with the reaction with CH_3Br :

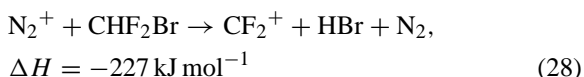
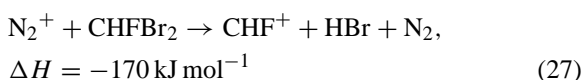
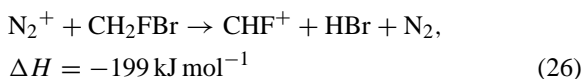


For the reaction of N_2^+ with $CHBrCl_2$, dissociative charge transfer leading to the Br^+ , CCl^+ , and $CHCl^+$ product ions is exothermic:



Reaction enthalpies for the above channels have been determined using $\Delta_f H(CHCl^+) = 1198 \text{ kJ mol}^{-1}$ and $\Delta_f H(CCl^+) = 1275 \text{ kJ mol}^{-1}$ reported by Rodriguez et al. [36]. For the reaction of N_2^+ with CH_2FBr , $CHFBr_2$, and CHF_2Br the following

dissociative charge transfer channels are exothermic:



Non-dissociative charge transfer to N_2^+ is only observed for two of the reactions, that with CH_2FBr and CHF_2Br , and then only with small branching ratios, 3 and 2%, respectively. For these two reactant molecules, the parent ion is observed for reactions with all reagent ions, with one exception. The reaction of O^+ with CHF_2Br results in only one product ion CHF_2^+ , although other dissociative charge transfer channels are exothermically available (see Table 5). Morris et al. [9], have also investigated the reaction of O^+ with CHF_2Br . In agreement with our observations, they do not observe the parent ion. However, contrary to our findings, they observed two product ions, compared to our one. Whilst their dominant product ion agrees with our only product ion, they observe another ion assigned to be CHF^+ with a branching percentage ratio of 44%. However, CHF^+ cannot be a result of a dissociative charge transfer because that route is endothermic ($\Delta H = 174 \text{ kJ mol}^{-1}$, with neutral products FBr and O), and there is no obvious exothermic chemical pathway.

Of the 56 reactions reported in this section, only 1 has been previously reported in the literature, O^+ with CHF_2Br [9]. All of the reagent ions react with the eight hydrogenated bromomethanes investigated with reaction rate coefficients at or close to the calculated (or expected) collisional value. The reaction mechanism is considered to be predominantly dissociative charge transfer. An inspection of the available photoelectron spectra for CH_3Br and CH_2Br_2 [35], and CH_2BrCl , CHBrCl_2 and CHBr_2Cl [37] indicates that many of the dissociative charge transfers must occur via a short-range interaction owing to small or zero

Franck–Condon factors linking the neutral reactant molecules to their various ionic states at the recombination energies of the reagent ions. The exceptions are the reactions of CO_2^+ , CO^+ and N_2^+ with CH_3Br , CO^+ and N^+ with CH_2Br_2 , N^+ with CH_2BrCl , and N_2^+ with CHBrCl_2 for which a good intensity is observed in the photoelectron spectra of the neutral molecules at these ions' recombination energies, and hence long-range dissociative charge transfer may be operative. We cannot be so definitive with respect to the dissociative charge transfer mechanism involving reactions with CH_2FBr , CHF_2Br , and CHFBr_2 , because no photoelectron spectra for these molecules have been reported in the literature.

3.3. The Group (iii) molecules: $\text{CF}_3\text{CF}_2\text{Br}$ and $\text{CF}_2\text{BrCF}_2\text{Br}$

A natural extension to the studies of the reactions of positive ions with partially and fully halogenated methanes is the investigations of the corresponding reactions with the halogenated ethanes. In this section the reactions of the reagent ions with two fully halogenated molecules ($\text{CF}_3\text{CF}_2\text{Br}$ and $\text{CF}_2\text{BrCF}_2\text{Br}$) are discussed. No previous positive ion–molecule reaction studies with either of these two molecules are reported in the literature, other than a study involving H_3O^+ by us [16]. The results of the reactions of H_2O^+ , N_2O^+ , O^+ , CO_2^+ , CO^+ , N^+ , and N_2^+ with $\text{CF}_3\text{CF}_2\text{Br}$ and $\text{CF}_2\text{BrCF}_2\text{Br}$ at 300 K are presented in Table 3. All of the reactions are efficient with $k_{\text{exp}} \geq 10^{-9} \text{ cm}^3 \text{ molecule}^{-1} \text{ s}^{-1}$. The recombination energies of the reagent ions exceed the ionisation potentials of $\text{CF}_3\text{CF}_2\text{Br}$ and $\text{CF}_2\text{BrCF}_2\text{Br}$. Thus, charge transfer is exothermically available, and it is found to be predominantly dissociative:



where $\text{X} = \text{F}$, CF_3 , Br or CF_2Br . Only the photoelectron spectrum of $\text{CF}_2\text{BrCF}_2\text{Br}$ is reported in the literature [38]. An inspection of this spectrum suggests that N_2O^+ , N^+ , and N_2^+ can possibly react via a long-range charge transfer mechanism with $\text{CF}_2\text{BrCF}_2\text{Br}$, because good Franck–Condon factors

Table 6

Reaction rate coefficients, the product ions, and the branching percentages for the reactions of H_2O^+ with $\text{CH}_3\text{CH}_2\text{Br}$, $\text{CH}_2\text{BrCH}_2\text{Cl}$, and $\text{CH}_2\text{BrCH}_2\text{Br}$ at 300 K

	$\text{CH}_3\text{CH}_2\text{Br}$ (10.28)	$\text{CH}_2\text{BrCH}_2\text{Cl}$ (10.67)	$\text{CH}_2\text{BrCH}_2\text{Br}$ (10.38)
H_2O^+ (12.61)	2.5 [3.1] CH_3CH_2^+ (69) $\text{CH}_3\text{CH}_2\text{Br}^+$ (31)	2.2 [1.9] $\text{CH}_2\text{CH}_2\text{Cl}^+$ (100)	1.9 [1.8] $\text{CH}_2\text{BrCH}_2^+$ (99) $\text{CH}_2\text{BrCH}_2\text{Br}^+$ (1)

The reaction rate coefficients, both experimental and calculated collisional (in square brackets), are given in units of $10^{-9} \text{ cm}^3 \text{ molecule}^{-1} \text{ s}^{-1}$. Product ion branching percentages are given in parentheses.

connect the ground state neutral reactant molecule to an ionic state at the recombination energies of these ions. The proposed reaction mechanism is therefore dissociative charge transfer via a short-range mechanism within an ion–molecule complex, i.e., short-range dissociative charge transfer is again the proposed favoured mechanism for the majority of the reactions.

The observation of C_2F_4^+ as a product ion from the reactions of O^+ , CO^+ , N^+ , and N_2^+ with $\text{CF}_2\text{BrCF}_2\text{Br}$ cannot be via reaction (29) in which a single bond is broken. If dissociative charge transfer is responsible for the C_2F_4^+ product ion, then both the carbon–bromine bonds need to be broken, and the proposed neutral product is Br_2 .

Non-dissociative charge transfer is observed for the majority of the reactions, but usually as a minor product channel. The exceptions to this are the reactions of H_2O^+ and N^+ with $\text{CF}_3\text{CF}_2\text{Br}$, for which $\text{CF}_3\text{CF}_2\text{Br}^+$ is observed to be a major product ion with a percentage branching ratio of 26 and 29%, respectively.

TPEPICO data on $\text{CF}_3\text{CF}_2\text{Br}$ and $\text{CF}_2\text{BrCF}_2\text{Br}$ would be useful in providing information on the available fragmentation channels from the ionic states, and thereby help to determine whether a dissociative charge transfer reaction process is occurring via a long-range or a short-range interaction.

3.4. Other reactions: H_2O^+ reactions with three bromine containing hydrogenated ethanes

An initial study of the reactions of positive ions with $\text{CH}_3\text{CH}_2\text{Br}$, $\text{CH}_2\text{BrCH}_2\text{Cl}$, and $\text{CH}_2\text{BrCH}_2\text{Br}$ are presented here. Results of the reactions of H_2O^+ with $\text{CH}_3\text{CH}_2\text{Br}$, $\text{CH}_2\text{BrCH}_2\text{Cl}$, and $\text{CH}_2\text{BrCH}_2\text{Br}$ are

presented in Table 6. The collisional rate coefficients have been determined using the Langevin method for reactions with $\text{CH}_2\text{BrCH}_2\text{Cl}$ and $\text{CH}_2\text{BrCH}_2\text{Br}$, because their dipole moments are unavailable. Comparisons of k_{exp} with k_{c} show that all three reactions are efficient. Non-dissociative charge transfer is observed for the reactions with $\text{CH}_3\text{CH}_2\text{Br}$ (31%) and (weakly) with $\text{CH}_2\text{BrCH}_2\text{Br}$ (1%). Dissociative charge transfer is the dominant channel for the reaction with these two molecules and is the only pathway for reaction with $\text{CH}_2\text{BrCH}_2\text{Cl}$. All three dissociative charge transfer channels involve ejection of atomic bromine. Similarly, the efficient reaction of O_2^+ with $\text{CH}_3\text{CH}_2\text{Br}$ led to two ion products [10]. $\text{CH}_3\text{CH}_2\text{Br}^+$ resulted from non-dissociative charge transfer (60%) and dissociative charge transfer led to CH_3CH_2^+ , with Br and O_2 as the assumed neutral products. That the non-dissociative charge transfer channel is the dominant reaction pathway is not surprising. The recombination energy of O_2^+ is 0.54 eV lower than that of H_2O^+ . The higher branching ratio for the non-dissociative charge transfer channel for O_2^+ compared to H_2O^+ is thus attributed to the lower energy deposited in $(\text{CH}_3\text{CH}_2\text{Br}^+)^*$. For the three reactions studied no product ions resulting from the loss of an H atom, and in the case of reaction with $\text{CH}_2\text{BrCH}_2\text{Cl}$, no Cl loss, were observed.

4. Concluding remarks

The results of a SIFT study of the reactions of H_2O^+ , N_2O^+ , O^+ , CO_2^+ , CO^+ , N^+ , and N_2^+ with the bromine containing molecules CF_3Br , CF_2Br_2 ,

CFBr₃, CF₂BrCl, CFB₂Cl, CBrCl₃, CH₃Br, CH₂Br₂, CH₂FBr, CHF₂Br, CHFBr₂, CH₂BrCl, CHBrCl₂, CHBr₂Cl, CF₃CF₂Br, and CF₂BrCF₂Br at 300 K have been described. The reactions of H₂O⁺ with CH₃CH₂Br, CH₂BrCH₂Cl, and CH₂BrCH₂Br have also been reported. This provides an extensive database on the positive ion chemistry of brominated molecules. All the reactions are rapid, and mostly proceed via dissociative charge transfer. The dissociative charge transfer is considered to be via a short-range interaction for the majority of reactions. Comparison of TPEPICO studies with the results from this investigation would be useful for confirming this proposal, as has been illustrated for the reactions with CF₃Br.

Acknowledgements

We are grateful to the Technological Plasmas Initiative Programme, EPSRC (Grant Reference: GR/L82083) for the financial support of this study.

References

- [1] Y. Ikezoe, S. Matsuoka, M. Takebe, A. Viggiano, Gas Phase Ion–Molecule Reaction Rate Coefficients Through 1986, Ion Reaction Research Group, The Mass Spectroscopy Society of Japan.
- [2] D.B. Graves, M.J. Kushner, J.W. Gallagher, A. Garscadden, G.S. Oehrlein, A.V. Phelps, B. Hui, C. Robertson, D.F. Morgan, Database Needs for Modeling and Simulation of Plasma Processing, National Academy Press, Washington, DC, 1996.
- [3] R.A. Morris, T.M. Miller, A.A. Viggiano, J.F. Paulson, S. Solomon, G.J. Reid, J. Geophys. Res. 100D (1995) 1287.
- [4] R.A. Morris, A.A. Viggiano, S.T. Arnold, J.F. Paulson, Int. J. Mass Spectrom. Ion Process. 148–151 (1995) 287.
- [5] G. Jarvis, C.A. Mayhew, R.P. Tuckett, J. Phys. Chem. A 100 (1996) 17166.
- [6] G.K. Jarvis, R.A. Kennedy, C.A. Mayhew, R.P. Tuckett, Int. J. Mass Spectrom. Ion Process. 202 (2000) 323.
- [7] R.A. Morris, A.A. Viggiano, J.M. Van Doren, J.F. Paulson, J. Phys. Chem. 96 (1992) 3051.
- [8] R.D. Thomas, R.A. Kennedy, C.A. Mayhew, P. Watts, J. Phys. Chem. A 101 (1997) 8489.
- [9] R.A. Morris, A.A. Viggiano, S.T. Arnold, J.F. Paulson, J.F. Liebman, J. Phys. Chem. 99 (1995) 5992.
- [10] P. Španel, D. Smith, Int. J. Mass Spectrom. 189 (1999) 213.
- [11] N.G. Adams, D. Smith, in: J.M. Farrar, W.H. Saunders (Eds.), Techniques for the Study of Ion–Molecule Reactions, Wiley, New York, 1988, p. 165.
- [12] D. Smith, N.G. Adams, Adv. Atom. Mol. Phys. 24 (1988) 1.
- [13] D. Smith, N.G. Adams, Int. J. Mass Spectrom. Ion. Phys. 21 (1976) 349.
- [14] W. Lindinger, F. Howorka, P. Lukac, S. Kuhn, H. Villinger, E. Alge, H. Ramler, Phys. Rev. A 23 (1981) 2319.
- [15] D. Smith, N.G. Adams, Phys. Rev. A 23 (1981) 2327.
- [16] R.A. Kennedy, C.A. Mayhew, R.D. Thomas, P. Watts, Int. J. Mass Spectrom. 223–224 (2003) 627.
- [17] T. Su, W.J. Chesnavich, J. Chem. Phys. 76 (1982) 5183.
- [18] G. Gioumousis, D.P. Stevenson, J. Chem. Phys. 29 (1959) 294.
- [19] D.R. Lide (Ed.), CRC Handbook of Chemistry and Physics, 82nd Edition, CRC Press, Boca Raton, FL, 2001.
- [20] R.A. Morris, J. Chem. Phys. 97 (1992) 2372.
- [21] W.B. Knighton, E.P. Grimsrud, J. Am. Chem. Soc. 114 (1992) 2336.
- [22] W.G. Mallard, P.J. Linstrom (Eds.), NIST Chemistry WebBook, NIST Standard Reference Database Number 69, February 2000, National Institute of Standards and Technology, Gaithersburg, MD (<http://webbook.nist.gov>).
- [23] S.J. Lias, J.E. Bartmess, J.F. Liebman, J.L. Holmes, R.D. Levin, W.G. Mallard, J. Phys. Chem. Ref. Data Suppl. 1 (1988) 17.
- [24] R.A. Morris, E.R. Brown, A.A. Viggiano, J.M. Van Doren, J.F. Paulson, V. Motevalli, Int. J. Mass Spectrom. Ion Process. 121 (1992) 95.
- [25] R.A. Morris, J.M. Van Doren, A.A. Viggiano, J.F. Paulson, J. Chem. Phys. 97 (1992) 173.
- [26] R.A. Morris, A.A. Viggiano, J.M. Van Doren, J.F. Paulson, J. Phys. Chem. 96 (1992) 2597.
- [27] J. Doucet, P. Sauvageau, C. Sandorfy, J. Chem. Phys. 58 (1973) 3708.
- [28] J. Doucet, R. Gilbert, P. Sauvageau, C. Sandorfy, J. Chem. Phys. 62 (1975) 366.
- [29] F.T. Chau, C.A. McDowell, J. Electron Spectrosc. Relat. Phenom. 6 (1975) 357.
- [30] I. Novak, T. Cvitaš, L. Klasinc, H. Güsten, J. Chem. Soc., Faraday Trans. 2 77 (1981) 2929.
- [31] F. Wang, and G.E. Leroi, Ann. Isr. Phys. Soc. 6 (1983) 210.
- [32] J.C. Creasey, D.M. Smith, R.P. Tuckett, K.R. Yoxall, K. Codling, P.A. Hatherly, J. Phys. Chem. 100 (1996) 4350.
- [33] G.K. Jarvis, R.A. Kennedy, C.A. Mayhew, R.P. Tuckett, Int. J. Mass Spectrom. 202 (2000) 32.
- [34] C. Lane, I. Powis, J. Phys. Chem. 97 (1993) 5803.
- [35] W. von Niessen, L. Åsbrink, G. Bieri, J. Electron Spectrosc. Relat. Phenom. 26 (1982) 173.
- [36] C.F. Rodriguez, D.K. Bohme, A.C. Hopkinson, J. Phys. Chem. 100 (1996) 2942.
- [37] I. Novak, T. Cvitaš, L. Klasinc, H. Güsten, J. Chem. Soc., Faraday Trans. 2 77 (1981) 2929.
- [38] F.T. Chau, C.A. McDowell, J. Phys. Chem. 80 (1976) 2923.